






Article

Sustainable Synthesis of Silver Nanoparticles Using Marine Algae for Catalytic Degradation of Methylene Blue

Chandra Kishore Somasundaram ¹, Raji Atchudan ^{2,*} , Thomas Nesakumar Jebakumar Immanuel Edison ² , Suguna Perumal ² , Rajangam Vinodh ³, Ashok K. Sundramoorthy ⁴ , Rajendran Suresh Babu ⁵ , Muthulakshmi Alagan ⁶ and Yong Rok Lee ^{2,*}

¹ Department of Biomedical Engineering, Saveetha School of Engineering, Saveetha Institute of Medical and Technical Sciences (SIMATS), Saveetha University, Chennai 602105, India; schandrakishore30@gmail.com

² School of Chemical Engineering, Yeungnam University, Gyeongsan 38541, Korea; jebakumar84@yu.ac.kr (T.N.J.I.E.); suguna.perumal@gmail.com (S.P.)

³ School of Electrical and Computer Engineering, Pusan National University, Busan 46241, Korea; vinoth6482@gmail.com

⁴ Department of Chemistry, SRM Institute of Science and Technology, Kattankulathur 603203, Tamil Nadu, India; ashokkus@srmist.edu.in

⁵ Laboratory of Experimental and Applied Physics, Centro Federal de Educação Tecnológica Celso Suckow da Fonseca (CEFET/RJ), Av. Maracanã 229, Rio de Janeiro 20271-110, Brazil; ryesbabu@gmail.com

⁶ Faculty of Information and Communication Science, University of Information Science and Technology “St. Paul the Apostle”, 6000 Ohrid, North Macedonia; almuthulakshmi@gmail.com

* Correspondence: atchudanr@yu.ac.kr (R.A.); yrlee@yu.ac.kr (Y.R.L.)



Citation: Somasundaram, C.K.; Atchudan, R.; Edison, T.N.J.I.; Perumal, S.; Vinodh, R.; Sundramoorthy, A.K.; Babu, R.S.; Alagan, M.; Lee, Y.R. Sustainable Synthesis of Silver Nanoparticles Using Marine Algae for Catalytic Degradation of Methylene Blue. *Catalysts* **2021**, *11*, 1377. <https://doi.org/10.3390/catal11111377>

Academic Editor:
Ioannis Konstantinou

Received: 27 October 2021
Accepted: 12 November 2021
Published: 15 November 2021

Publisher's Note: MDPI stays neutral with regard to jurisdictional claims in published maps and institutional affiliations.



Copyright: © 2021 by the authors. Licensee MDPI, Basel, Switzerland. This article is an open access article distributed under the terms and conditions of the Creative Commons Attribution (CC BY) license (<https://creativecommons.org/licenses/by/4.0/>).

Abstract: Herein, *Sargassum coreanum* (marine algae)-mediated silver nanoparticles (AgNPs) were successfully synthesized by a simple reduction method. The synthesized AgNPs were characterized using ultraviolet-visible spectroscopy, attenuated total reflection Fourier transformed infrared spectroscopy, X-ray diffractometry, field emission scanning electron microscopy (FESEM) with energy-dispersive X-ray (EDX) spectroscopy, and high-resolution transmission electron microscopy (HR-TEM) analysis. The acquired colloidal AgNPs were strongly absorbed around 420 nm and displayed brown color under visible light. The XRD pattern of AgNPs exposed their face-centered cubic geometry along with crystalline nature. The HRTEM images of synthesized AgNPs confirmed the mean particle size of 19 nm with a distorted spherical shape, and the calculated interlayer distance (d-spacing value) was about 0.24 nm. Further, the catalytic degradation of methylene blue using sodium borohydride and AgNPs was monitored using UV-vis spectroscopy. The result revealed that AgNPs performed as a superior catalyst, which completely degraded MB in 20 min. The rate constant for MB degradation was calculated to be 0.106 min^{-1} , demonstrating that the marine algae-mediated AgNPs had outstanding catalytic activity. This approach is easy and environmentally benign, which can be applied for environmental-based applications such as dye degradation and pollutant detoxification.

Keywords: *Sargassum coreanum*; marine algae; silver nanoparticles; methylene blue; catalytic degradation

1. Introduction

In recent days, the impact of industrialization has resulted in a significant rise in dyes, insecticides, phenols, and other organic pollutants with potentially toxic by-products [1]. Among various industries such as paper, textile, plastic, rubber, and cosmetics utilize dyes extensively. Nearly every day, a large portion of the world's dye output is discharged into the seas during the dying process [2]. Reverse osmosis, adsorption, flocculation, coagulation, ultrafiltration, and flocculation are non-destructive traditional water treatment methods that simply transfer pollutants from one stage to another, resulting in a secondary

waste issue [3]. Because these compounds are resistant to natural degradation, their ever-increasing quantities in the environment, particularly in water sources, are a cause of worry for society and regulatory agencies all over the globe [4]. For the total degradation of dyes, most typical water treatment procedures such as membrane filtration, adsorption, and chemical treatment are inadequate [5,6]. On the other hand, these technologies produce secondary pollutants such as poisonous gases and sludge as solid wastes that must be treated subsequently. As an alternative, catalysis plays a major role in the complete degradation of organic pollutants [6–9].

Methylene blue (MB) is a blue cationic thiazine dye widely used in dyeing cotton, wool, and silk [10]. It has three mesomeric configurations, with the positive charge located on either the amine nitrogen atom or the sulfur atom [11]. Because of its bright color and toxicity, the presence of this dye in the effluent can pose a serious hazard viz., stomach pain, vomiting, and dysentery to individuals and indirectly affect the ecosystem [12]. Physical methodologies such as adsorption [13], precipitation [14], and reverse osmosis [15]; chemical techniques such as oxidation [16] and reduction [17]; and biological methods such as aerobic and anaerobic intervention have all been often used to clean dye-containing wastewaters [18]. On the other hand, overdosing on MB can produce central nervous system toxicity; therefore, its breakdown is both environmentally and physiologically essential. Noble metal nanoparticles, such as Au, Ag, Pd, Pt, and Cu, have been extensively studied for efficient catalytic reduction and decoloration of dyes in an aqueous phase at room temperature [19–23]. These catalysts have already demonstrated significant characteristics such as increased efficiency, eco-friendly processing, and easy implementation. Among them, silver nanoparticles (AgNPs) are a popular redox catalyst that requires less activation energy and provides a unique electron transfer reaction route. Consequently, AgNPs promote electron transport during the process and assist in the degradation of the MB dye [24].

AgNPs are significant materials that have been widely explored [25]. These nanoscale materials are used in biosensing [26], catalysis [27], imaging [28], nanodevice [29], drug delivery [30], and medicine [31] because they have superior electrical, optical, and biological capabilities [32]. The usage of AgNPs as a nanocatalyst in the context of environmental degradation of MB is perhaps the most notable of these applications [33]. Despite the fact that many synthetic approaches in material synthesis are widely reported, researchers throughout the globe are still looking for acceptable biomaterials for the biosynthesis of AgNPs [32,34]. Though several physicochemical approaches may be used to create AgNPs, they are both costly and possibly hazardous to the environment. On the other hand, chemical procedures use harmful compounds as reducing agents, liquid hydrocarbons, and non-biodegradable stabilizing agents, posing a risk to the environment and biodiversity [32]. In an environmentally friendly approach, the use of biological entities such as microbes and plant extracts might replace chemical and physical processes for the green synthesis of AgNPs [35].

The use of biological species to synthesize nanomaterials is gaining popularity since biological approaches are less costly, nontoxic, and ecologically friendly “green chemistry” procedures [36]. When opposed to a microbial-based method, using plants and plant extracts to synthesize nanoparticles has the benefit of eliminating the time-consuming procedure of preserving cell cultures [37]. Biogenic synthesis can create vast numbers of nanoparticles free of contaminants, have a well-defined size and shape, and have a low environmental effect [38]. In this present investigation, we use the extract from *Sargassum coreanum* (marine algae) to synthesize AgNPs and their application toward the degradation of MB. Terpenoids, volatile hydrocarbons, oxylipins, phlorotannins, and steroids are among the secondary metabolites produced by marine algae [39]. Several of these compounds have been shown to have a wide range of biological activities, including antibacterial, cytotoxic, and antioxidant behavior, as well as inhibitory action against a variety of enzymes [40]. Reducing sugars in the marine algae extract allows the Ag ions to be readily reduced to AgNPs, while the alkaloids and amino acids from the extract

stabilize the AgNPs by electrostatic interaction that helps against agglomeration, lead better nanoparticle stability [41]. Polysaccharides, polyphenols, protein content, and other phytoconstituents are also found in the *Sargassum coreanum*. The reduction of AgNO_3 to AgNPs is mainly due to these phytoconstituents [42–46]. Furthermore, *Sargassum coreanum* is abundant in water bodies and is readily available at no cost. As a result, the *Sargassum coreanum* was utilized as a perfect reducing and stabilizing agent for the synthesis of AgNPs towards MB degradation.

2. Results and Discussion

2.1. Characterization of the Prepared Silver Nanoparticles

One of the extensively adopted techniques for structural characterization of metal nanoparticles is UV-Vis spectroscopy. Figure 1 depicts the UV-vis spectra of algae extract and prepared AgNPs. The algae extract shows two major absorbance peaks in the UV-region at 220 and 275 nm attributed to the $\pi-\pi^*$ and $n-\pi^*$ transitions of phytoconstituents, while the synthesized AgNPs mainly absorbed in the visible region at 420 nm and display brown color due to the surface plasmon resonance of AgNPs. This result indicated the formation of colloidal AgNPs [47]. The absorption curve morphologies indicate that the nanoparticles were well disseminated and spherical in shape [48]. Because the surface-to-volume ratio rises with decreasing particle size, it is well understood that the size and shape of Ag NPs have a significant impact on their optical characteristics [49]. Moreover, the surface plasmon resonance due to the obvious interaction among incoming light and electrons present in the conduction band on the AgNPs surface are considered to be responsible for these nanoparticles to be substantially absorbed in the UV-vis range [47].

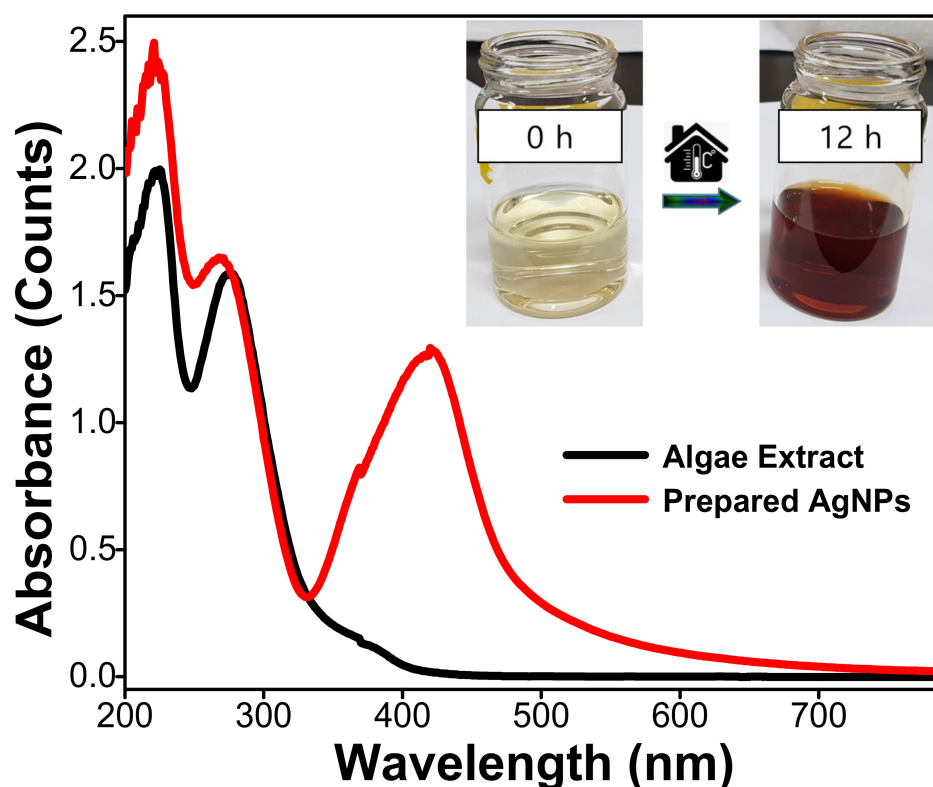


Figure 1. UV-vis spectra of algae extract and prepared Ag NPs.

ATR-FTIR is a valuable technique for determining the role of functional groups attached to the metal particles. FTIR studies were used in this investigation to detect the functional groups that may be responsible for capping and stabilizing the Ag NPs, thereby accessing their quality and nature, as shown in Figure 2a. The vibrations of the $-\text{OH}$, $-\text{NH}$, and $-\text{CH}_2$ functional groups present over the AgNPs, having the origin from algae extract,

exhibited strong absorption bands around at 3400, 3220, and 2935 cm^{-1} , respectively [50]. The O–H stretching vibration of water molecules adsorbed on the AgNPs surface caused a high absorption around 3400 cm^{-1} . The additional bands occurred at 1714, 1610, 1454, 1202, and 1035 cm^{-1} , perhaps owing to the stretching of the $\text{C}=\text{O}$, $\text{C}=\text{C}$, $\text{C}-\text{N}$, $\text{C}-\text{OH}$, and $\text{C}-\text{O}-\text{C}$ groups, respectively. Furthermore, the bands representing $\text{O}-\text{H}/-\text{N}-\text{H}$ bending vibrations occurred at 1325 cm^{-1} . These functional groups may play an important role in AgNPs' green production. During the synthesis, the presence of hydroxyl and carboxylate groups enhances the complexation of Ag ions. Individual Ag ions were then reduced to elemental Ag by in situ oxidation of hydroxyl and carbonyl groups. The FTIR substantiates this postulated process as well. However, the probable process is unknown and has to be investigated extensively.

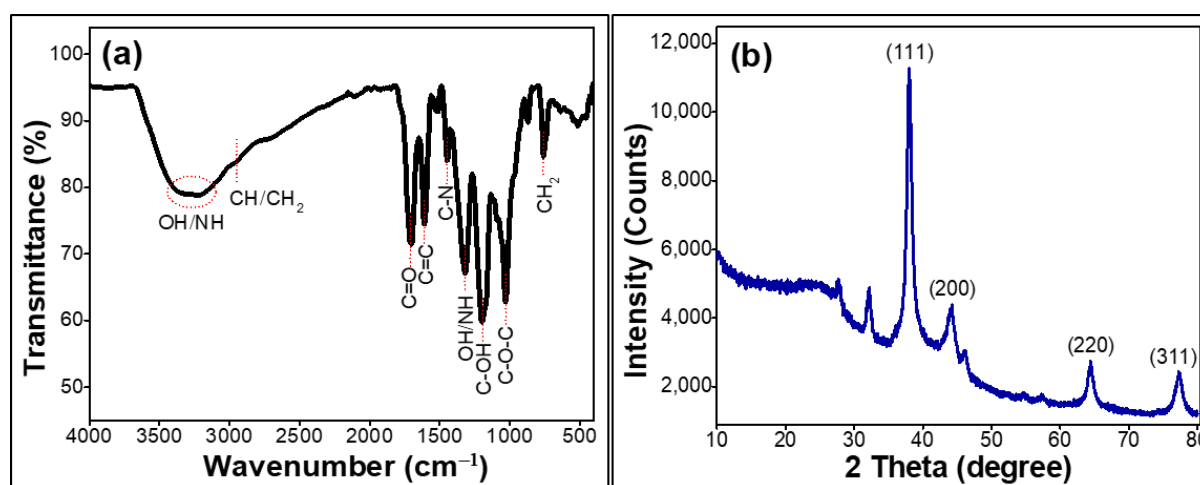


Figure 2. ATR-FTIR and XRD studies of AgNPs. (a) ATR-FTIR spectrum and (b) XRD pattern of prepared AgNPs.

The XRD spectrum of AgNPs synthesized with algae extract is shown in Figure 2b. The values of synthesized AgNPs in the spectrum ($2\theta =$) are 38.0° , 44.2° , 64.4° , and 77.2° respectively, which correlate to the diffractions of the (1 1 1), (2 0 0), (2 2 0) and (3 1 1) crystalline planes of face-centered cubic of Ag (JCPDS File No. 00-004-0783) [51]. The (1 1 1) plane has the highest intensity, implying that the produced AgNPs are widely dispersed in this plane. The crystallite size of synthesized AgNPs was also determined using Scherrer's formula from the full width at half maximum (FWHM) of the peak representing (1 1 1) plane [52]. Notable, the size of produced AgNPs was determined to be 17 nm. Additionally, to calculate the lattice spacing, the peak corresponding to the (1 1 1) crystalline plane was selected and found to be 0.24 nm.

The surface morphology and elemental composition of the AgNPs synthesized from *Sargassum coreanum* were examined by FESEM with EDX mapping analysis, as shown in Figure 3. The micrographs (Figure 3a–d) reveal that AgNPs formed are nearly spherical and are found to be in aggregates. The phytoconstituents present in the extract of *Sargassum coreanum* that forms a layer over these AgNPs may be considered to be responsible for this aggregate behavior of AgNPs. During the FESEM sample preparation, these AgNPs were coated over silicon (Si) substrates and kept for drying to remove the moisture present. Consequently, these AgNPs also tend to get aggregated during the expelling of water from the samples during the drying process. The area of AgNPs shown in Figure 3d was selected for elemental mapping and shown as (Figure 3e–h). From the mapping, the presence of elements Ag, carbon (C), oxygen (O), and nitrogen (N) are visible from the colors magenta, green, red, and yellow, respectively. Among these elements, Ag species were densely and uniformly dispersed as majority constitutes compared to other elements. The source of Ag is from AgNO_3 , which was used as the precursor for synthesizing the same. The results from XRD well coincide with this observation regarding the formation of crystalline AgNPs. At the same time, the other elements C, O, and N have their origin from the

phytoconstituents present in *Sargassum coreanum* extract. In addition, the EDX spectrum shown in Figure 3i illustrates the elemental composition of prepared AgNPs. The spectrum depicts energy peaks corresponding to Ag, C, O, N, Si, and Platinum (Pt). Here, Si has its source from Si wafer used as a substrate for sample preparation, whereas Pt is used as its ohmic contact.

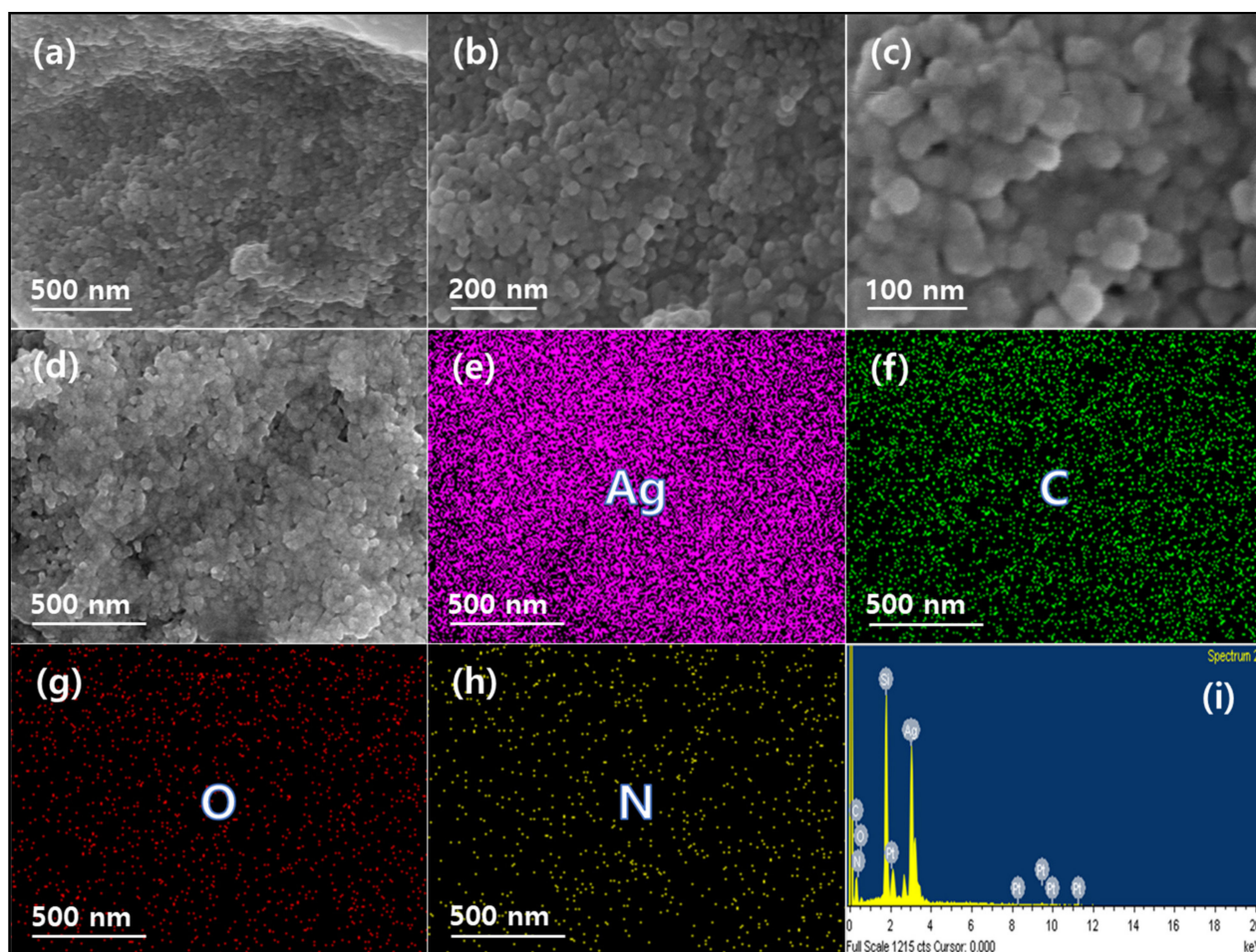


Figure 3. FESEM studies of AgNPs. (a–d) FESEM images with different magnifications of prepared AgNPs and the corresponding elemental mapping of (e) Ag, (f) C, (g) O, (h) N. (i) EDX spectrum of prepared AgNPs.

The morphology and size of green synthesized AgNPs were determined by TEM/HRTEM analysis, as shown in Figure 4. AgNPs are observed to be distinct particles with almost spherical shapes. Interestingly, no remarkable agglomeration in the particles was seen due to the presence of various functional groups attached to the surface of AgNPs, as confirmed from the ATR-FTIR analysis. From the TEM images, it was noticed that the AgNPs were engulfed by a thin amorphous layer, presumed to be the presence of left-over extract surrounding the nanoparticles. The particle size distribution graph (inset of Figure 4a) reveals the size of AgNPs was in the range of 10–30 nm. Based on Gaussian fitting, the particle size of AgNPs was determined to have an average size of 19 nm. Moreover, the lattice fringes are clear from the HRTEM image (Figure 4d), and the d-spacing was determined to be 0.24 nm, which conforms to the AgNPs (1 1 1) plane. Noteworthy, this observation well coincides with XRD [53]. The crystallinity of the produced nanoparticles was further corroborated by high-resolution pictures that revealed distinct lattice fringes.

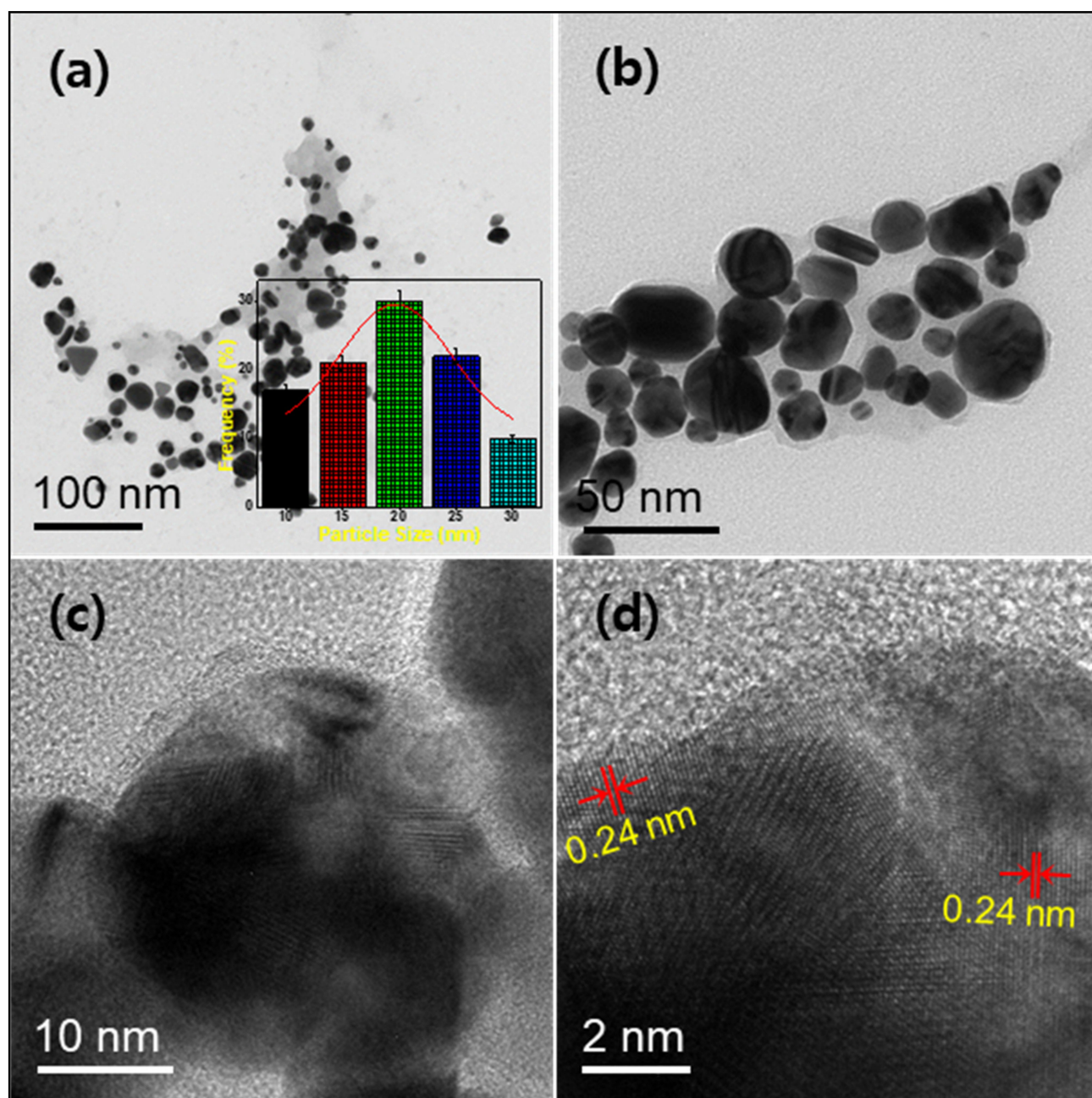


Figure 4. HRTEM images of AgNPs. (a,b) TEM images (inset (a) is a particle size distribution graph) and (c,d) HRTEM images of prepared AgNPs.

The plausible mechanism of AgNPs synthesis from the extract of *Sargassum coreanum* is illustrated in Figure 5. The extract of *Sargassum coreanum* has several phytoconstituents such as polysaccharides, polyphenol contents, and so on [54]. Furthermore, lignans are the key constituents in the marine algae extracts, which encompass metabolites such as ethyl acetate, petroleum ether, and methanolic extract can be responsible for the bioreduction reaction of Ag ions (AgNO_3 to AgNPs) and nanoparticle (AgNPs) stabilization [55].

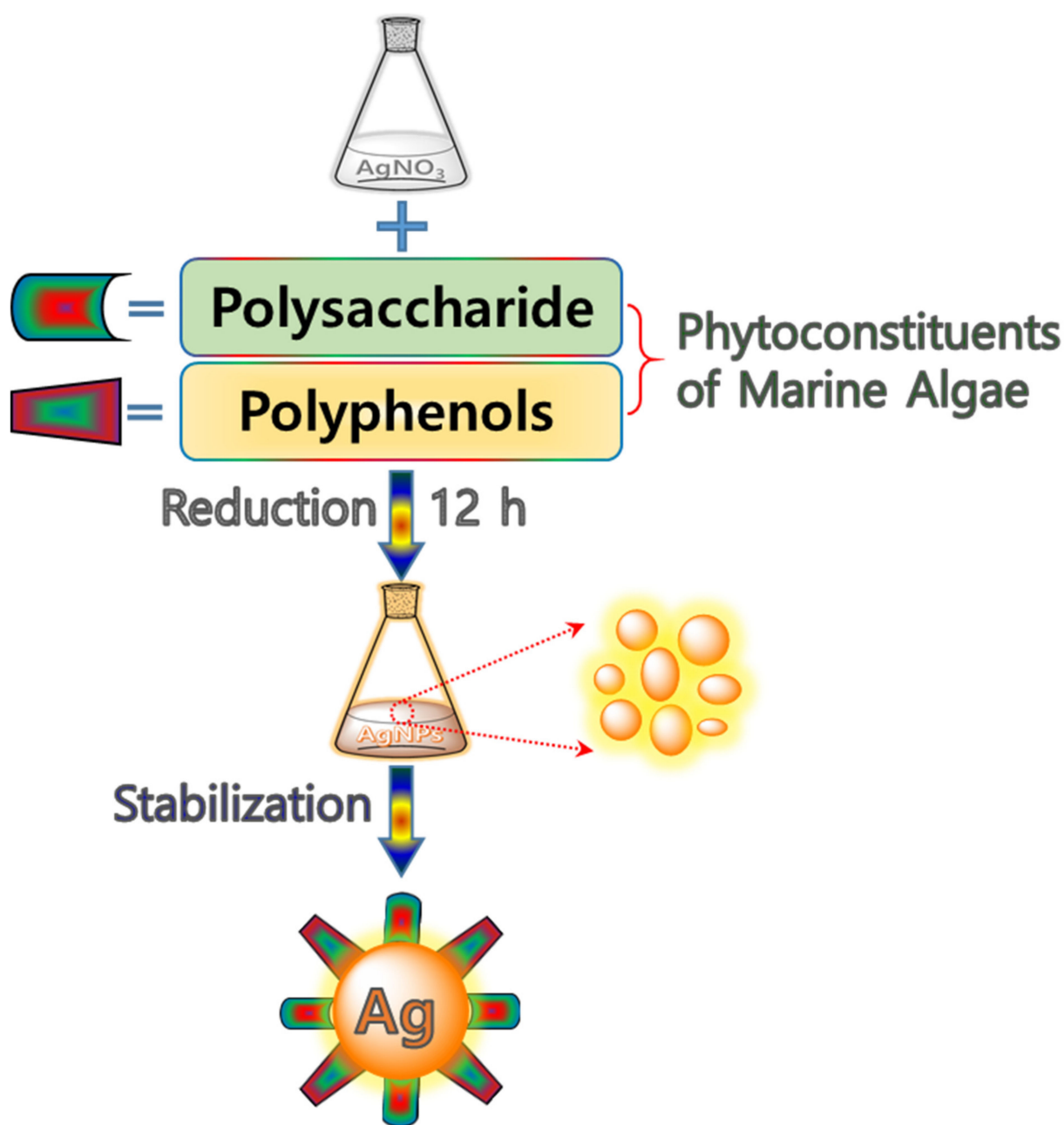


Figure 5. A plausible mechanism of silver nanoparticles synthesis from the extract of *Sargassum coreanum*.

2.2. Dye Degradation Efficiency of the Prepared Silver Nanoparticles

UV–vis spectroscopy was used to investigate the catalytic activity of produced AgNPs on the degradation of MB, as shown in Figure 6a. Aqueous MB's UV–vis spectrum displays two peaks in the visible region at 612 and 665 nm [56]. The degradation of MB did not happen in the control reaction when NaBH_4 was used solely, i.e., without AgNPs. Moreover, when AgNPs were added to solutions containing MB and NaBH_4 , MB degradation began very quickly, as seen by the progressive disappearance of blue color and decline in UV–vis spectra. Figure 6a shows the UV–vis spectra of MB degradation as a function of time. The absorbance intensity of MB steadily dropped with the addition of AgNPs + NaBH_4 as the reaction time increased, indicating that produced AgNPs have significant catalytic efficiency. The MB degradation was finished within 20 min, as evidenced by the decolorization of blue color and decrease in absorption intensity. For better visualization and confirmation in the transition of MB color from blue to transparent, a photographic image of the process

is shown in Figure S1. For comparison, Figure 6b shows the effect of MB degradation with time using only AgNPs, based on UV-vis absorbance. Interestingly, there were no significant changes in the intensity of absorbance peaks, indicating no occurrence of MB degradation. Figure 6c shows the degrading efficiency of MB for three set of reactions ((MB + NaBH₄), (MB + AgNPs + NaBH₄), and (MB + AgNPs)) at different reaction durations. It was very clear from the graph, MB degradation did not happen with (MB + AgNPs) and (MB + NaBH₄) combination reaction, as indicated by the merging of the two lines with zero slope. Whereas the linear red line represents degradation using (MB + AgNPs + NaBH₄), confirming complete degradation (>99%) of MB was accomplished in 20 min. Notable, from the pseudo-first-order kinetic plot shown in Figure 6d, the degradation of MB by AgNPs with NaBH₄ is predicted to be pseudo-first-order. Additionally, the degradation of dye MB and response time were shown to have a linear correlation. The linear line's mathematical equation is $Y = -0.106X + 0.083$ ($Y = mX + C$), where m -line's slope, C -line's intercept. The linearity factor (R^2) was determined as 0.981. The rate constant (k) for the degradation of MB using AgNPs was derived from the straight-line gradient value based on the previously reported literature [37,57–59] and is 0.106 min^{-1} . Moreover, the MB degrading efficiency was calculated to be >99%. Consequently, the biosynthesized AgNPs from algae proved to be a reliable and potential candidate to degrade MB.

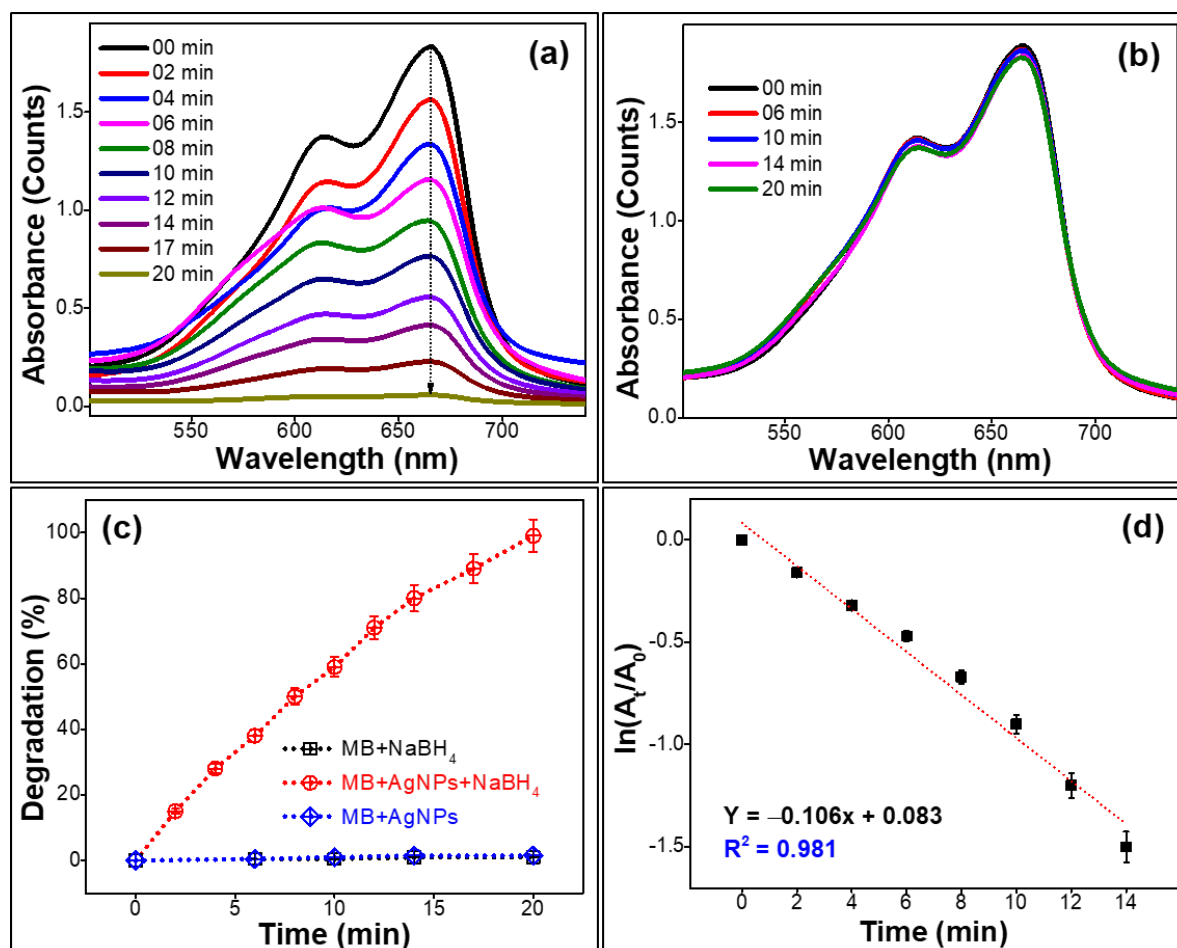


Figure 6. Degradation studies. (a) UV-vis absorbance of methylene blue with prepared silver nanoparticles and NaBH₄ at different reaction times, (b) UV-vis absorbance of methylene blue with prepared AgNPs at different reaction time (c) degradation efficiency (%) of silver nanoparticles towards the methylene blue, and (d) pseudo-first-order kinetic plot for the degradation of methylene blue.

A plausible mechanism of methylene blue degradation in the presence of the prepared AgNPs is illustrated in Figure 7. In general, MB is made stable and colorless in an aqueous

solution by reducing MB into leuco-methylene blue (LMB) and MBH_2^+ [19]. In an oxidizing state, MB becomes blue and is easily reduced by reducing agents to the colorless, leuco forms (degraded product, DP) [60]. The Langmuir–Hinshelwood model was used to describe the possible mechanism for AgNPs aided catalytic breakdown of MB [61]. NaBH_4 serves as both an electron donor and a hydrogen supplier in this scenario. AgNPs act as an intermediate to transfer the electrons between BH_4^- ion and MB because of their high negative potential (-1.8 V vs. NHE) [33,62]. After adding NaBH_4 to a solution having MB and AgNPs, the BH_4^- ion from NaBH_4 and MB molecules adsorb on the AgNPs surface, resulting in instantaneous electron and hydrogen transport. Diffusion among adsorbed molecules causes desorption of the colorless degraded by-product that might give additional catalytic sites for the breakdown of MB attributable to AgNPs wide surface area.

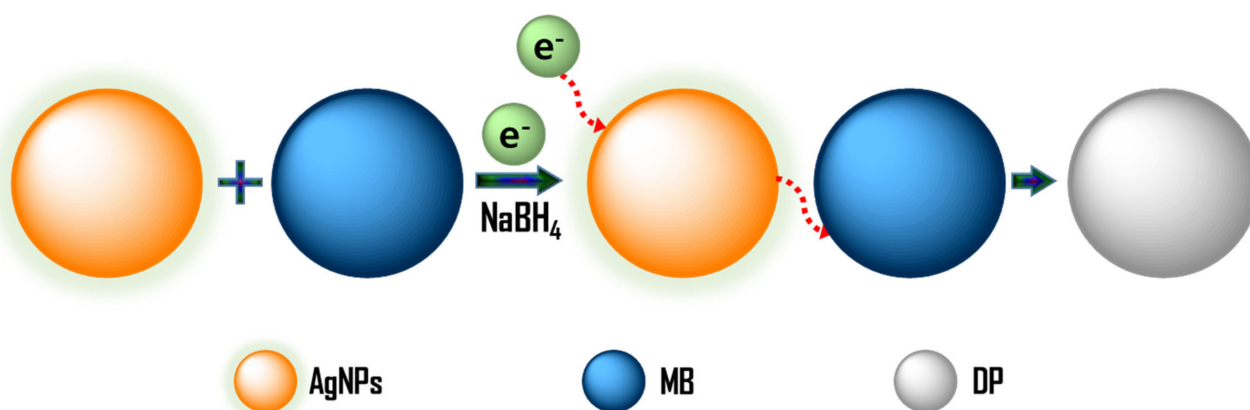


Figure 7. A plausible mechanism of methylene blue degradation in the presence of the prepared silver nanoparticles.

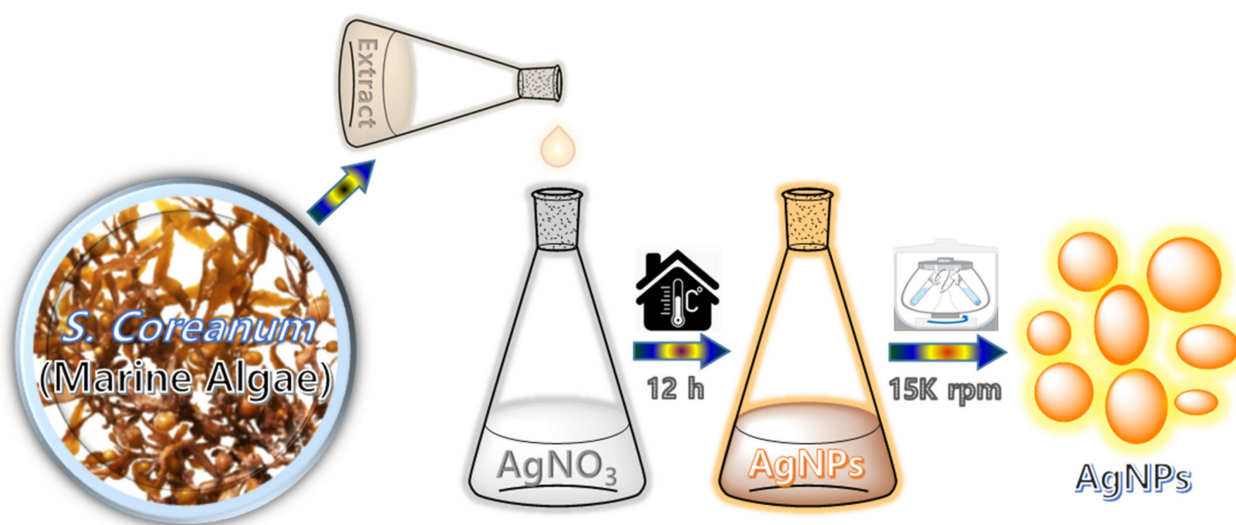
3. Experimental

3.1. Materials

Sargassum coreanum (marine algae) was collected from the sea-source area (Beach), Busan, Republic of Korea. Silver nitrate (AgNO_3), sodium borohydride (NaBH_4), and methylene blue were purchased from Sigma-Aldrich, Seoul, Republic of Korea. All the chemicals were used as received. Distilled water was used throughout this work.

3.2. Preparation of Silver Nanoparticles

AgNPs were prepared from the marine algae extract, as shown in Scheme 1. The marine algae were well cleaned with water, dried, and finely powdered. 5 g of powdered algae in 100 mL of distilled water was heated at 80°C for 30 min, cooled to room temperature, and filtered with Whatman 40 filter paper. The resulting filtrate was employed to prepare AgNPs, where 5 mL of the aqueous extract was added to 20 mL of 0.1 M AgNO_3 solutions at room temperature (25°C) to produce AgNPs. The color of the AgNO_3 solution changed from colorless to brown after 12 h, indicating the occurrence of AgNPs. To separate the AgNPs, the final solution was subjected to centrifugation at 15,000 r.p.m. After centrifugation, the obtained supernatant AgNPs was taken further for the MB degradation.



Scheme 1. Preparation of AgNPs using marine algae at room temperature.

3.3. Catalytic Degradation Measurements

The prepared AgNPs were employed as a catalyst in the degradation of methylene blue (MB) using NaBH_4 , which was done in a quartz UV cuvette. Then, 2 mL (50 μM) of MB was mixed with 0.95 mL (0.005 M) of aqueous NaBH_4 and 0.05 mL of AgNPs. The degradation dynamics of MB were observed using an OPTIZEN 3220UV spectrophotometer. The degradation efficiency (%) and the reaction rate constant of degradation (pseudo-first-order) were calculated using the following Equations (1) and (2).

$$\text{Degradation efficiency (\%)} = \left(\frac{A_0 - A_t}{A_0} \right) \times 100 \quad (1)$$

$$\text{Pseudo - first - order } (-kt) = \ln \left(\frac{A_t}{A_0} \right) \quad (2)$$

where, A_0 and A_t are the absorbance of MB at 0 and t time, respectively. k is the degradation reaction rate constant.

4. Conclusions

To sum up, we present a green synthesis of AgNPs from marine algae extract that is easy, quick, and economical. Employing algae as a template, we were able to produce AgNPs quickly from AgNO_3 . The algae act as a framework for both reduction and stability of the AgNPs formed. The approach follows the “green chemistry” principle. The formation of AgNPs has been demonstrated using UV-vis spectroscopy, ATR-FTIR, XRD, and TEM/HRTEM. The synthesized AgNPs with the average particle size of 19 nm were purely crystalline, as confirmed by HRTEM analysis. With reference to the ATR-FTIR and HRTEM data, it was discovered that phytoconstituents in the extract prevent AgNPs from agglomeration and make them very stable. The rate constant for MB degradation was calculated to be 0.106 min^{-1} , which proved AgNPs from marine algae extracts to possess excellent catalytic activity for the complete degradation of MB in a short interval of time of 20 min. Moreover, AgNPs are bestowed with maximum MB degradation efficiency of >99%. In the near future, these AgNPs prepared from marine algae extract are attractive prospects for various pharmacological, biological, and environmental applications due to their rapid and efficient surface reactivity.

Supplementary Materials: The following are available online at <https://www.mdpi.com/article/10.3390/catal11111377/s1>, Instrumentation methods and catalytic degradation measurement of the prepared AgNPs, Figure S1: Visual observation of methylene blue degradation using AgNPs.

Author Contributions: Investigation and writing-original draft, C.K.S.; Conceptualization, data curation, formal analysis, investigation and writing-original draft, R.A.; Methodology and resources, T.N.J.I.E.; Writing-review & editing, S.P.; Formal analysis and validation, R.V.; Validation and visualization, A.K.S.; Investigation and validation, R.S.B.; Investigation and visualization, M.A.; Project administration and supervision, Y.R.L. All authors equally contributed to this work. All authors have read and agreed to the published version of the manuscript.

Funding: This work was supported by the National Research Foundation of Korea (NRF) grant funded by the Korean government MSIT (2021R1A2B5B02002436).

Institutional Review Board Statement: Not applicable.

Informed Consent Statement: Not applicable.

Data Availability Statement: No data availability.

Acknowledgments: Authors thank the National Research Foundation of Korea (NRF) for providing financial support.

Conflicts of Interest: The authors declare no conflict of interest.

References

1. Antoci, A.; Galeotti, M.; Sordi, S. Environmental pollution as engine of industrialization. *Commun. Nonlinear. Sci.* **2018**, *58*, 262–273. [\[CrossRef\]](#)
2. Kang, L.; Du, H.L.; Du, X.; Wang, H.T.; Ma, W.L.; Wang, M.L.; Zhang, F.B. Study on dye wastewater treatment of tunable conductivity solid-waste-based composite cementitious material catalyst. *Desalin. Water Treat.* **2018**, *125*, 296–301. [\[CrossRef\]](#)
3. Lakherwal, D. Adsorption of heavy metals: A review. *Int. J. Environ. Res. Dev.* **2014**, *4*, 41–48.
4. Mir, N.; Khan, A.; Umar, K.; Muneer, M. Photocatalytic Study of a Xanthene Dye Derivative, Phloxine B in Aqueous Suspension of TiO₂: Adsorption Isotherm and Decolourization Kinetics. *Energy Environ. Focus* **2013**, *2*, 208–216. [\[CrossRef\]](#)
5. Kim, S.; Chen, J.P.; Ting, Y. Study on feed pretreatment for membrane filtration of secondary effluent. *Sep. Purif. Technol.* **2002**, *29*, 171–179. [\[CrossRef\]](#)
6. Umar, K.; Haque, M.M.; Mir, N.A.; Farooqi, I.H.; Muneer, M. Titanium Dioxide-mediated Photocatalysed Mineralization of Two Selected Organic Pollutants in Aqueous Suspensions. *J. Adv. Oxid. Technol.* **2013**, *16*. [\[CrossRef\]](#)
7. Umar, K.; Ibrahim, M.N.M.; Ahmad, A.; Rafatullah, M. Synthesis of Mn-doped TiO₂ by novel route and photocatalytic mineralization/intermediate studies of organic pollutants. *Res. Chem. Intermed.* **2019**, *45*, 2927–2945. [\[CrossRef\]](#)
8. Mir, N.A.; Haque, M.; Khan, A.; Umar, K.; Muneer, M.; Vijayalakshmi, S. Semiconductor Mediated Photocatalysed Reaction of Two Selected Organic Compounds in Aqueous Suspensions of Titanium Dioxide. *J. Adv. Oxid. Technol.* **2012**, *15*, 380–391. [\[CrossRef\]](#)
9. Umar, K.; Dar, A.A.; Haque, M.; Mir, N.; Muneer, M. Photocatalysed decolourization of two textile dye derivatives, Martius Yellow and Acid Blue 129, in UV-irradiated aqueous suspensions of Titania. *Desalin. Water Treat.* **2012**, *46*, 205–214. [\[CrossRef\]](#)
10. Mills, A.; Hazafy, D.; Parkinson, J.; Tuttle, T.; Hutchings, M.G. Effect of alkali on methylene blue (C.I. Basic Blue 9) and other thiazine dyes. *Dye. Pigment.* **2011**, *88*, 149–155. [\[CrossRef\]](#)
11. Ratova, M.; Marcelino, R.B.P.; De Souza, P.P.; Amorim, C.C.; Kelly, P.J. Reactive Magnetron Sputter Deposition of Bismuth Tungstate Coatings for Water Treatment Applications under Natural Sunlight. *Catalysts* **2017**, *7*, 283. [\[CrossRef\]](#)
12. Othman, N.H.; Alias, N.H.; Shahrudin, M.Z.; Abu Bakar, N.F.; Him, N.R.N.; Lau, W.J. Adsorption kinetics of methylene blue dyes onto magnetic graphene oxide. *J. Environ. Chem. Eng.* **2018**, *6*, 2803–2811. [\[CrossRef\]](#)
13. Rafatullah, M.; Sulaiman, O.; Hashim, R.; Ahmad, A. Adsorption of methylene blue on low-cost adsorbents: A review. *J. Hazard. Mater.* **2010**, *177*, 70–80. [\[CrossRef\]](#)
14. Yang, Z.; Li, M.; Yu, M.; Huang, J.; Xu, H.; Zhou, Y.; Song, P.; Xu, R. A novel approach for methylene blue removal by calcium dodecyl sulfate enhanced precipitation and microbial flocculant GA1 flocculation. *Chem. Eng. J.* **2016**, *303*, 1–13. [\[CrossRef\]](#)
15. Li, H.; Lin, Y.; Luo, Y.; Yu, P.; Hou, L. Relating organic fouling of reverse osmosis membranes to adsorption during the reclamation of secondary effluents containing methylene blue and rhodamine B. *J. Hazard. Mater.* **2011**, *192*, 490–499. [\[CrossRef\]](#)
16. Dutta, K.; Mukhopadhyay, S.; Bhattacharjee, S.; Chaudhuri, B. Chemical oxidation of methylene blue using a Fenton-like reaction. *J. Hazard. Mater.* **2001**, *84*, 57–71. [\[CrossRef\]](#)
17. Begum, R.; Najeeb, J.; Sattar, A.; Naseem, K.; Irfan, A.; Al-Sehemi, A.G.; Farooqi, Z.H. Chemical reduction of methylene blue in the presence of nanocatalysts: A critical review. *Rev. Chem. Eng.* **2019**, *36*, 749–770. [\[CrossRef\]](#)
18. Bedekar, P.A.; Kshirsagar, S.D.; Gholave, A.R.; Govindwar, S.P. Degradation and detoxification of methylene blue dye adsorbed on water hyacinth in semi continuous anaerobic–aerobic bioreactors by novel microbial consortium-SB. *RSC Adv.* **2015**, *5*, 99228–99239. [\[CrossRef\]](#)
19. Suvith, V.; Philip, D. Catalytic degradation of methylene blue using biosynthesized gold and silver nanoparticles. *Spectrochim. Acta Part A Mol. Biomol. Spectrosc.* **2014**, *118*, 526–532. [\[CrossRef\]](#)

20. Gong, P.; Li, B.; Kong, X.; Shakeel, M.; Liu, J.; Zuo, S. Hybridizing hierarchical zeolite with Pt nanoparticles and graphene: Ternary nanocomposites for efficient visible-light photocatalytic degradation of methylene blue. *Microporous Mesoporous Mater.* **2018**, *260*, 180–189. [\[CrossRef\]](#)
21. Hu, H.; Shao, M.; Zhang, W.; Lu, L.; Wang, A.H.; Wang, S. Synthesis of Layer-Deposited Silicon Nanowires, Modification with Pd Nanoparticles, and Their Excellent Catalytic Activity and Stability in the Reduction of Methylene Blue. *J. Phys. Chem. C* **2007**, *111*, 3467–3470. [\[CrossRef\]](#)
22. Sangpour, P.; Hashemi, F.; Moshfegh, A.Z. Photoenhanced degradation of methylene blue on cosputtered M: TiO₂ (M= Au, Ag, Cu) nanocomposite systems: A comparative study. *J. Phys. Chem. C* **2010**, *114*, 13955–13961. [\[CrossRef\]](#)
23. Malik, A.; Hameed, S.; Siddiqui, M.J.; Haque, M.M.; Umar, K.; A Khan, A.; Muneer, M. Electrical and Optical Properties of Nickel- and Molybdenum-Doped Titanium Dioxide Nanoparticle: Improved Performance in Dye-Sensitized Solar Cells. *J. Mater. Eng. Perform.* **2014**, *23*, 3184–3192. [\[CrossRef\]](#)
24. Tripathi, R.; Kumar, N.; Shrivastav, A.; Singh, P.; Shrivastav, B. Catalytic activity of biogenic silver nanoparticles synthesized by Ficus panda leaf extract. *J. Mol. Catal. B Enzym.* **2013**, *96*, 75–80. [\[CrossRef\]](#)
25. Yaqoob, A.A.; Umar, K.; Ibrahim, M.N.M. Silver nanoparticles: Various methods of synthesis, size affecting factors and their potential applications—a review. *Appl. Nanosci.* **2020**, *10*, 1369–1378. [\[CrossRef\]](#)
26. Fan, M.; Thompson, M.; Andrade, M.L.; Brolo, A.G. Silver Nanoparticles on a Plastic Platform for Localized Surface Plasmon Resonance Biosensing. *Anal. Chem.* **2010**, *82*, 6350–6352. [\[CrossRef\]](#)
27. Jiang, Z.-J.; Liu, C.-Y.; Sun, L.-W. Catalytic Properties of Silver Nanoparticles Supported on Silica Spheres. *J. Phys. Chem. B* **2005**, *109*, 1730–1735. [\[CrossRef\]](#)
28. Caro, C.; Castillo, P.M.; Klippstein, R.; Pozo, D.; Zaderenko, A.P. Silver Nanoparticles: Sensing and Imaging Applications. *Silver Nanoparticles* **2010**. [\[CrossRef\]](#)
29. Mohanpuria, P.; Rana, N.K.; Yadav, S.K. Biosynthesis of nanoparticles: Technological concepts and future applications. *J. Nanopart. Res.* **2008**, *10*, 507–517. [\[CrossRef\]](#)
30. Prasher, P.; Sharma, M.; Mudila, H.; Gupta, G.; Sharma, A.K.; Kumar, D.; Bakshi, H.A.; Negi, P.; Kapoor, D.N.; Chellappan, D.K.; et al. Emerging trends in clinical implications of bio-conjugated silver nanoparticles in drug delivery. *Colloid Interface Sci. Commun.* **2020**, *35*, 100244. [\[CrossRef\]](#)
31. Pantic, I. Application of silver nanoparticles in experimental physiology and clinical medicine: Current status and future prospects. *Rev. Adv. Mater. Sci.* **2014**, *37*, 15–19.
32. Beyene, H.D.; Werkneh, A.A.; Bezabh, H.K.; Ambaye, T.G. Synthesis paradigm and applications of silver nanoparticles (AgNPs), a review. *Sustain. Mater. Technol.* **2017**, *13*, 18–23. [\[CrossRef\]](#)
33. Edison, T.N.J.I.; Atchudan, R.; Kamal, C.; Lee, Y.R. Caulerpa racemosa: A marine green alga for eco-friendly synthesis of silver nanoparticles and its catalytic degradation of methylene blue. *Bioprocess Biosyst. Eng.* **2016**, *39*, 1401–1408. [\[CrossRef\]](#) [\[PubMed\]](#)
34. De Lima, R.; Seabra, A.; Durán, N. Silver nanoparticles: A brief review of cytotoxicity and genotoxicity of chemically and biogenically synthesized nanoparticles. *J. Appl. Toxicol.* **2012**, *32*, 867–879. [\[CrossRef\]](#)
35. Hebbalalu, D.; Lalley, J.; Nadagouda, M.N.; Varma, R.S. Greener Techniques for the Synthesis of Silver Nanoparticles Using Plant Extracts, Enzymes, Bacteria, Biodegradable Polymers, and Microwaves. *ACS Sustain. Chem. Eng.* **2013**, *1*, 703–712. [\[CrossRef\]](#)
36. Park, Y. New Paradigm Shift for the Green Synthesis of Antibacterial Silver Nanoparticles Utilizing Plant Extracts. *Toxicol. Res.* **2014**, *30*, 169–178. [\[CrossRef\]](#)
37. Edison, T.N.J.I.; Atchudan, R.; Karthik, N.; Balaji, J.; Xiong, D.; Lee, Y.R. Catalytic degradation of organic dyes using green synthesized N-doped carbon supported silver nanoparticles. *Fuel* **2020**, *280*, 118682. [\[CrossRef\]](#)
38. Mohammed, A.E.; Al-Qahtani, A.; Al-Mutairi, A.; Al-Shamri, B.; Aabed, K.F. Antibacterial and Cytotoxic Potential of Biosynthesized Silver Nanoparticles by Some Plant Extracts. *Nanomaterials* **2018**, *8*, 382. [\[CrossRef\]](#)
39. Yang, X.; Kang, M.-C.; Lee, K.-W.; Kang, S.-M.; Lee, W.-W.; Jeon, Y.-J. Antioxidant activity and cell protective effect of loliolide isolated from Sargassum ringgoldianum subsp. coreanum. *ALGAE* **2011**, *26*, 201–208. [\[CrossRef\]](#)
40. Chang, H.W.; Jang, K.H.; Lee, D.; Kang, H.R.; Kim, T.-Y.; Lee, B.H.; Choi, B.W.; Kim, S.; Shin, J. Monoglycerides from the brown alga Sargassum sagamianum: Isolation, synthesis, and biological activity. *Bioorganic Med. Chem. Lett.* **2008**, *18*, 3589–3592. [\[CrossRef\]](#)
41. Venkatesan, J.; Kim, S.-K.; Shim, M.S. Antimicrobial, Antioxidant, and Anticancer Activities of Biosynthesized Silver Nanoparticles Using Marine Algae Ecklonia cava. *Nanomaterials* **2016**, *6*, 235. [\[CrossRef\]](#)
42. Massironi, A.; Morelli, A.; Grassi, L.; Puppi, D.; Braccini, S.; Maisetta, G.; Esin, S.; Batoni, G.; Della Pina, C.; Chiellini, F. Ulvan as novel reducing and stabilizing agent from renewable algal biomass: Application to green synthesis of silver nanoparticles. *Carbohydr. Polym.* **2018**, *203*, 310–321. [\[CrossRef\]](#)
43. Acharya, D.; Satapathy, S.; Yadav, K.K.; Somu, P.; Mishra, G. Systemic Evaluation of Mechanism of Cytotoxicity in Human Colon Cancer HCT-116 Cells of Silver Nanoparticles Synthesized Using Marine Algae Ulva lactuca Extract. *J. Inorg. Organomet. Polym. Mater.* **2021**, 1–10. [\[CrossRef\]](#)
44. Khalifa, K.; Hamouda, R.; Hanafy, D.; Hamza, A. In vitro antitumor activity of silver nanoparticles biosynthesized by marine algae. *Dig. J. Nanomater. Biostruct.* **2016**, *11*, 213–221.
45. Selvaraj, P.; Neethu, E.; Rathika, P.; Jayaseeli, J.P.R.; Jermy, B.R.; AbdulAzeez, S.; Borgio, J.F.; Dhas, T.S. Antibacterial potentials of methanolic extract and silver nanoparticles from marine algae. *Biocatal. Agric. Biotechnol.* **2020**, *28*, 101719. [\[CrossRef\]](#)

46. Hamouda, R.A.; El-Mongy, M.A.; Eid, K.F. Comparative study between two red algae for biosynthesis silver nanoparticles capping by SDS: Insights of characterization and antibacterial activity. *Microb. Pathog.* **2019**, *129*, 224–232. [\[CrossRef\]](#)
47. Singaravelan, R.; Alwar, S.B.S. Electrochemical synthesis, characterisation and phytogenic properties of silver nanoparticles. *Appl. Nanosci.* **2015**, *5*, 983–991. [\[CrossRef\]](#)
48. Logar, M.; Jancar, B.; Suvorov, D. In situ synthesis of Ag nanoparticles in polyelectrolyte multilayers. *Nanotechnology* **2007**, *18*, 325601. [\[CrossRef\]](#)
49. Zhang, Z.; Shao, C.; Sun, Y.; Mu, J.; Zhang, M.; Zhang, P.; Guo, Z.; Liang, P.; Wang, C.; Liu, Y. Tubular nanocomposite catalysts based on size-controlled and highly dispersed silver nanoparticles assembled on electrospun silica nanotubes for catalytic reduction of 4-nitrophenol. *J. Mater. Chem.* **2012**, *22*, 1387–1395. [\[CrossRef\]](#)
50. Kora, A.J.; Arunachalam, J. Green Fabrication of Silver Nanoparticles by Gum Tragacanth (*Astragalus gummifer*): A Dual Functional Reductant and Stabilizer. *J. Nanomater.* **2012**, *2012*, 1–8. [\[CrossRef\]](#)
51. Darroudi, M.; Ahmad, M.B.; Abdullah, A.H.; Ibrahim, N.A. Green synthesis and characterization of gelatin-based and sugar-reduced silver nanoparticles. *Int. J. Nanomed.* **2011**, *6*, 569–574. [\[CrossRef\]](#)
52. Lanje, A.S.; Sharma, S.J.; Pode, R.B. Synthesis of silver nanoparticles: A safer alternative to conventional antimicrobial and antibacterial agents. *J. Chem. Pharm. Res.* **2010**, *2*, 478–483.
53. Philip, D. Honey mediated green synthesis of silver nanoparticles. *Spectrochim. Acta Part A Mol. Biomol. Spectrosc.* **2010**, *75*, 1078–1081. [\[CrossRef\]](#)
54. Hakim, M.M.; Patel, I.C. A review on phytoconstituents of marine brown algae. *Future J. Pharm. Sci.* **2020**, *6*, 1–11. [\[CrossRef\]](#)
55. Kasithevar, M.; Saravanan, M.; Prakash, P.; Kumar, H.; Ovais, M.; Barabadi, H.; Shinwari, Z.K. Green synthesis of silver nanoparticles using *Alysicarpus monilifer* leaf extract and its antibacterial activity against MRSA and CoNS isolates in HIV patients. *J. Interdiscip. Nanomed.* **2017**, *2*, 131–141. [\[CrossRef\]](#)
56. Joseph, S.; Mathew, B. Microwave-assisted green synthesis of silver nanoparticles and the study on catalytic activity in the degradation of dyes. *J. Mol. Liq.* **2015**, *204*, 184–191. [\[CrossRef\]](#)
57. Liu, X.; Liang, M.; Liu, M.; Su, R.; Wang, M.; Qi, W.; He, Z. Highly Efficient Catalysis of Azo Dyes Using Recyclable Silver Nanoparticles Immobilized on Tannic Acid-Grafted Eggshell Membrane. *Nanoscale Res. Lett.* **2016**, *11*, 1–9. [\[CrossRef\]](#) [\[PubMed\]](#)
58. Sharma, K.; Singh, G.; Kumar, M.; Bhalla, V. Silver nanoparticles: Facile synthesis and their catalytic application for the degradation of dyes. *RSC Adv.* **2015**, *5*, 25781–25788. [\[CrossRef\]](#)
59. Gola, D.; Kriti, A.; Bhatt, N.; Bajpai, M.; Singh, A.; Arya, A.; Chauhan, N.; Srivastava, S.K.; Tyagi, P.K.; Agrawal, Y. Silver nanoparticles for enhanced dye degradation. *Curr. Res. Green Sustain. Chem.* **2021**, *4*, 100132. [\[CrossRef\]](#)
60. Jamjoum, H.A.A.; Umar, K.; Adnan, R.; Razali, M.R.; Ibrahim, M.N.M. Synthesis, Characterization, and Photocatalytic Activities of Graphene Oxide/metal Oxides Nanocomposites: A Review. *Front. Chem.* **2021**, *9*. [\[CrossRef\]](#) [\[PubMed\]](#)
61. Panacek, A.; Prucek, R.; Hrbac, J.; Nevečná, T.j.; Steffkova, J.; Zboril, R.; Kvitek, L. Polyacrylate-assisted size control of silver nanoparticles and their catalytic activity. *Chem. Mater.* **2014**, *26*, 1332–1339. [\[CrossRef\]](#)
62. Edison, T.N.J.I.; Lee, Y.R.; Sethuraman, M.G. *Caulerpa racemosa*: Green synthesis of silver nanoparticles using *Terminalia cuneata* and its catalytic action in reduction of direct yellow-12 dye. *Spectrochim. Acta A.* **2016**, *161*, 122–129. [\[CrossRef\]](#)